Magazine of Civil Engineering

ISSN 2712-8172

journal homepage: http://engstroy.spbstu.ru/

DOI: 10.34910/MCE.101.8

Strength of concrete columns reinforced with Glass fiber reinforced polymer

N.P. Duy*[a], V.N. Anh[a], D.V. Hiep[b], N.M.T. Anh[a]

[a] Mientrung University of Civil Engineering, Tuyhoa, Phuyen, Vietnam

[b] Hanoi Architectural University, Thanhxuan, Hanoi, Vietnam

** E-mail: nguyenphanduy@muce.edu.vn*

Keywords: Finite element, glass fiber reinforced polymer (GFRP), reinforced concrete column, Abaqus, concentric compression

Abstract. Due to low compressive strength and low compressive elastic modulus in comparison with these in tension, GFRP reinforcement is often used for bending elements and is rarely used for compressive structures. In this paper, the authors used finite element (FE) method based on Abaqus software to evaluate the axial load-carrying capacity of GFRP reinforced concrete (RC) columns under varying concrete grades, GFRP reinforcement ratios and tie configurations. The model of the specimens is developed using concrete damage plastic (CDP) model and linear elastic material model for GFRP bar. The consistence of the FE method is verified by the experimental results of a series of columns that tested by current authors. The analytical results show that the selected numerical method can accurately predict the behavior as well as the ultimate capacity of the columns. From simulation results, it is clear that the contribution of GFRP to the load-carrying capacity is considerable in columns with low concrete grades. While using higher concrete grades, the contribution of GFRP decrease, at concrete grade B60, contribution of GFRP is almost unimportant (2.74 %). Influence of tie spacing on load-bearing capacity of columns is also investigated. Accordingly, reducing tie spacing leads to increase load-carrying capacity. Based on study results, the authors recommend to limit tie spacing less than eight times of the GFRP bar diameter.

1. Introduction

Nowadays the low durability problem could be solved by applying the new type of reinforcement in concrete structures i.e. the FRP reinforcement. The FRP reinforcement bar includes several different types as Glass Fiber Reinforced Polymer (GFRP), Carbon Fiber Reinforced Polymer (CFRP), Aramid Fiber Reinforced Polymer (AFRP), Basalt Fiber Reinforced Polymer (BFRP). The most popular is GFRP bar because of low price. In corrosive environments, the GFRP bar is considered a good substitute material for steel reinforcement. Compared to steel bar, GFRP is a material with many advantages such as corrosion resistance, high tensile strength, light weight, low electrical conductivity. Besides the advantages, it also has certain disadvantages, one of those is low compressive strength and compressive modulus of elasticity. Therefore, GFRP is mainly used to resist tensile load in tension zone of reinforced concrete structures [1, 2].

In order to expand the field of using GFRP reinforcement, especially for compressive elements of structures, many researchers have conducted study on GFRP RC columns under concentrically axial load. The goal of previous studies mainly focused on: evaluating the effect of longitudinal GFRP reinforcement on bearing capacity of columns; failure modes; the influence of configuration of GFRP transverse reinforcement on the behavior of columns and developing formulas to determine the load-carrying capacity etc. [3−11]. In these previous researches [3−11], it was showed that, when replacing the longitudinal steel bars with the GFRP bars by the same amount, the axial load-carrying capacity of GFRP concentrically RC columns decreases by 13 %–16 %. In GFRP RC columns, GFRP bars contribute about 3 %–10 % of the total load-carrying capacity. The increase of main GFRP reinforcement ratio boosts the ductility of cross section which has a significant effect on ultimate strain (to 19 %) and ultimate loads (to 22 %) of columns. Study results of Ehab M. Lotfy [5] indicated that, with the main reinforcement ratio up to 1.7 %, load-carrying capacity and

Duy, N.P., Anh, V.N., Hiep, D.V., Anh, N.M.T. Strength of concrete columns reinforced with Glass fiber reinforced polymer. Magazine of Civil Engineering. 2021. 101(1). Article No. 10108. DOI: 10.18720/MCE.101.8

reinforcement ratio follows a linear trend. Similarly, the author et al. [16] experimentally proved that, with the main reinforcement ratio up to 3.2 %, load-carrying capacity and reinforcement ratio follows a linear trend.

With the help of powerful commercial FE software, the FE modeling and analysis process is becoming increasingly efficient. Turvey and Zhang [12] conducted experiments and numerical simulations to study failure process after the loss of stability of RC columns reinforced with GFRP bars, using Abaqus software and generalized beam theory. In another study, F. Nunes et al. [13] carried out experiments and simulations of 3 series of I-section column from GFRP under eccentric compression. The results showed an excellent match between the experimental and numerical study results of the load-bearing capacity and the type of failures. Zhong Tao et al. [14] adjusted the FE model to simulate high-strength concrete filled steel tube under axial compression. In this model, the authors have adjusted the parameters in the CDP model for concrete, the modified model is more flexible and gives good convergence with the experimental results. Mohamed Elchalakani et al. [15] used CDP model to simulate GFRP RC columns in Abaqus. It can be seen from the results that the load-displacement response of simulations to experiments is in good agreement, the predicted *N-M* strength interaction diagrams are consistent with the experimental diagrams.

In general, the experimental data on the behavior of GFRP RC columns under axial load is relatively large. However, there are still some issues that have not been paid attention or just partially studied such as the influence of GFRP reinforcement ratios on the load-carrying capacity of the column; contribution of GFRP to load-carrying capacity of RC columns with different concrete grades and the influence of GFRP tie spacings on the load-bearing capacity of the columns. The current research work has been carried out to further investigate these issues using the nonlinear FE model method in Abaqus software. To achieve research objectives, the authors simulate the behavior of GFRP RC columns with different concrete grades, tie spacings and GFRP reinforcement ratios by using the CDP model and linear stress-strain behavior of GFRP in both tension and compression. From the simulation results, the axial load-concrete strain and axial load-displacement curves of columns under increasing static loading are presented and commented.

2. Methods

2.1. Experimental study program

To verify and adjust the parameters of the numerical model of GFRP RC columns, the authors used the previous experimental results of six short GFRP RC columns under axial load [16]. The size of the short columns was 150×150×600 mm. The average compressive strength of concrete determined by the test results of three 150×150×150 mm cubic specimens at 28th day is given in Table 1. The material properties of GFRP bars are also given in Table 1.

Table 1. Details of short GFRP RC column specimens [16].

Column ID	Long. reinf.			Tie		L_f/d_f	R_m,	R_f,	E_f,	R_{fc},	E_{fc},
	Bars	A_f, mm^2	μ_f, %	Bars	Spacing, mm		MPa	MPa	MPa	MPa	MPa
C1-4F6-F6S100	4F6	81.6	0.37	F6	100	16.67	29.9				
C2-4F12-F6S50	4F12	360.0	1.62	F6	50	4.17	32.2				
C3-4F12-6S100	4F12	360.0	1.62	F6	100	8.33	32.2				
C4-4F12-6S200	4F12	360.0	1.62	F6	200	16.67	32.2	970	44300	581	27930
C5-4F14-6S100	4F14	510.4	2.29	F6	100	7.14	30.3				
C6-8F12-6S100	8F12	720.0	3.24	F6	100	8.33	33.2				

F (d_f), mm is nominal diameter of GFRP bar; S (L_f), mm is tie spacing; A_f and μ_f are the area and percentage of longitudinal reinforcement respectively. R_m is the average compressive strength (cube 150×150×150 mm) at the age of 28 days. R_f and E_f are respectively, tensile strength and elastic modulus under tension of GFRP bar, R_{fc} and E_{fc} are respectively, compressive strength and elastic modulus under compression of GFRP bar

Tested columns differ in longitudinal reinforcement ratios μ_f and tie spacings S. The geometry, the reinforcement details of all column specimens are shown in Figure 1 and Table 1. In order to prevent crushing at the ends of column, thereby ensure failure at the middle of the column, the two ends of the columns are reinforced with steel nets. The purpose of the experiment is to build the axial strain versus axial load, as well as to determine the load-carrying capacity of the columns. The test setup and instrumentation employed to investigate the compression behavior of the GFRP RC columns are showed on Figure 2.

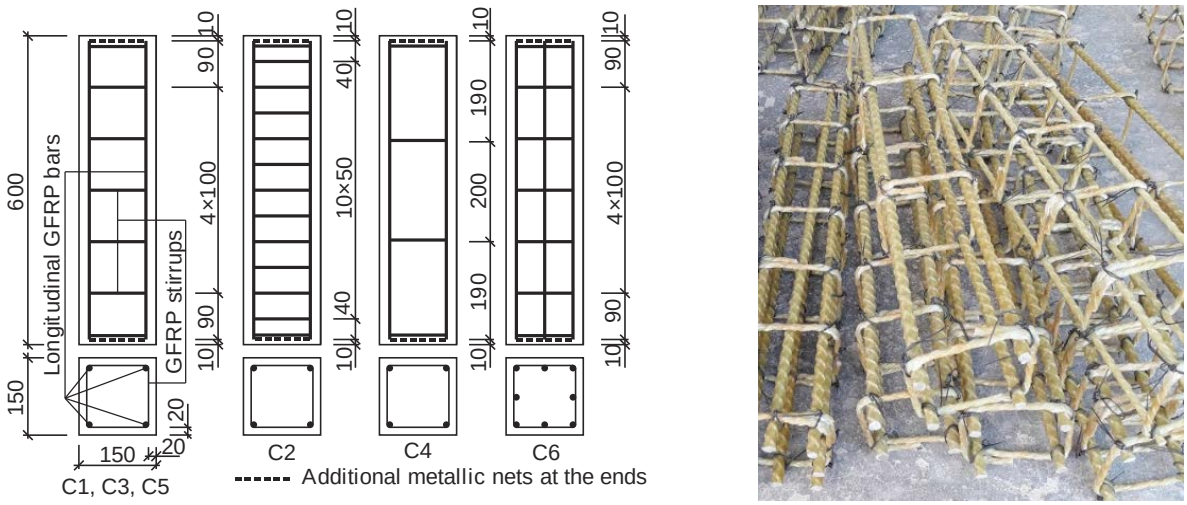

Figure 1. Details and configuration of the tested GFRP RC columns (units: mm).

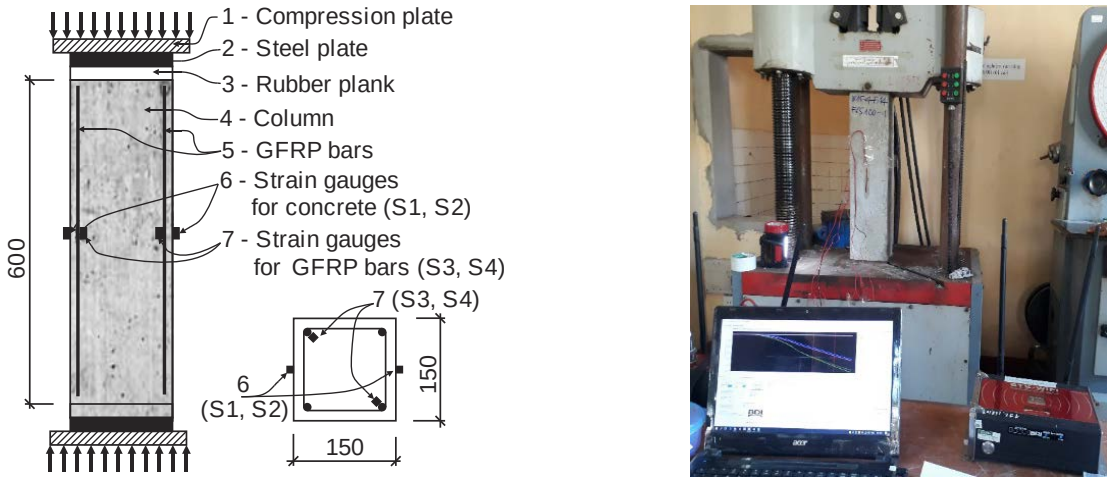

a) Schematic diagram **b) Actual**

Figure 2. Test setup and instrumentation for testing GFRP RC columns.

Loading of the column is applied on a testing machine of 100 tons. The columns were supported at both ends with two pairs of 8 mm thick steel plates. To fill the gaps between the steel plates and the surfaces of specimens, ensure uniform distribution of the applied load across the cross section and avoid eccentricity during loading, the authors used two rubber planks.

2.2. Numerical modeling and verification of numerical models

2.2.1. Numerical modeling

a) Describing structural parts and choosing element types

Abaqus software has a rich FE library, so selecting the appropriate element types for each component is necessary to simulate the column as close as possible to reality. In this paper, the eight-noded solid elements C3D8R with reduced integration is selected for concrete, steel plates and longitudinal GFRP bars, while GFRP stirrups is represented with two-noded linear truss element (T3D2).

b) Material properties

Concrete: full stress-strain diagram of concrete is displayed on Figure 3. It is seen that behavior of concrete is divided into two stages: elastic stage and inelastic stage. Under compression, elastic stage of concrete is built according to Model Code 2010 [17] and this stage is characterized by a secant modulus E_0 corresponding to a stress of $0.4f_{cm}$ and Poisson's ratio $\mu_c = 0.2$. Under tension, elastic stage of concrete is represented with E_0 and concrete tensile stress $f_{tm}=0.3016f_{ck}^{2/3}$. For the inelastic stage of concrete in both tension and compression, concrete damaged plasticity (CDP) model proposed by J. Lubliner et al. [18], J. Lee, G.L. Fenves [19] with some modifications according to B. Alfarah et al. [20] is employed. In Abaqus, plastic failure stage is declared through the following coefficients: ratio of second stress invariants on tensile and compressive meridians k_c=0.7; the ratio of biaxial compressive yield strength and uniaxial compressive yield strength f_{b0}/f_{c0}=1.16; the dilatancy angle of concrete ψ=13°; the eccentricity of plastic potential surface ϵ=0.1.

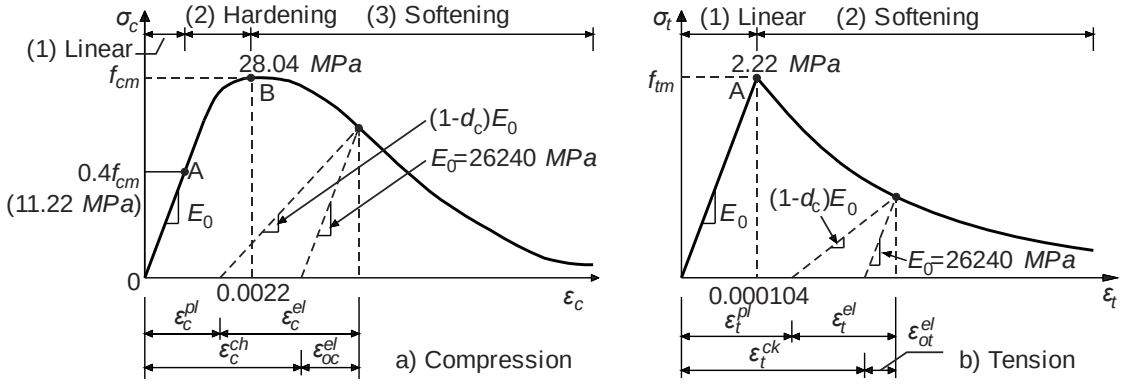

Figure 3. CDP model for concrete with R_m=32 *MPa* [18–20].

GFRP for longitudinal and transverse reinforcement: GFRP bar used in this experiment is provided by FRP VIETNAM., JSC [21]. Under tension, linear elastic model until failure based on the tensile test [22] is used to describe the behavior of GFRP (Figure 4 a). Under compression, the stress-strain diagram is built based on the Qasim S. Khan's proposal [23] and the results of tensile test mentioned above. Accordingly, the stress-strain diagram also has linear type as shown on Figure 4 b. According to the experimental results of GFRP bars in compression conducted by O.S. Al Ajarmeh et al. [24], slenderness ratio (L_f/d_f) affected significantly the failure behavior of GFRP bars in compression. With the $L_f/d_f \leq 8$, the compressive strength of GFRP is stable, in case $L_f/d_f > 8$, the compressive strength of GFRP reduces linearly. From the experimental research results by these authors, slenderness ratio does not affect significantly on the compressive elastic modulus. Therefore, in this study if $L_f/d_f \leq 8$, the compressive stress-strain relationship is used as shown in Figure 4 b , for the case of $L_f/d_f > 8$ a reduction in compressive stress and axial strain proposed in [24] is employed.

Steel plates (at the ends of columns) are made from CT3 steel and modeled with bi-linear elasto-plastic material properties without hardening stage (Figure 5). Steel plate uses CT3 material according to GOST 380–89. It is noted that the perfect bond between the GFRP bars and concrete is assumed.

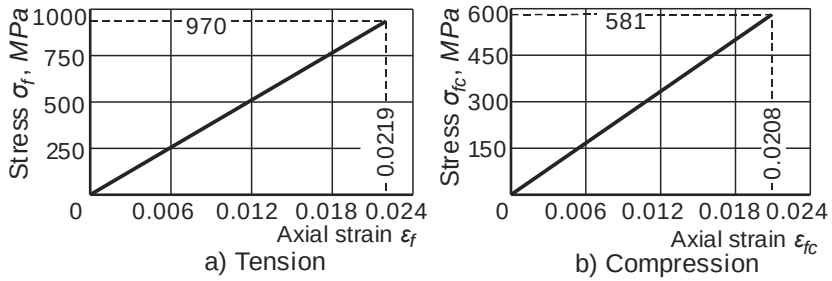

Figure 4. Stress-strain diagram of GFRP bars [22–24].

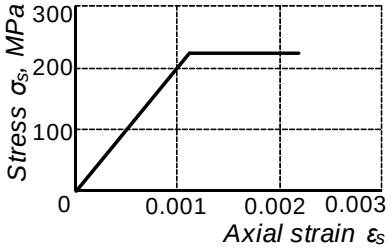

Figure 5. Stress-strain diagram of steel for plates.

c) Assembly of element parts: in Abaqus, each element of columns (concrete; steel plate; longitudinal GFRP bars; stirrups) is built independently in its local coordinate systems. Therefore, it is necessary to use assembly function to assemble discrete components to form a complete model. Figure 6a shows a complete model of column after assembly.

d) Conditions of interaction: in order to ensure the collaboration of all separate parts of the model, it is necessary to connect them together. Abaqus program provides different types of interaction. For GFRP RC columns, the interactions are as follows: tie constraint is used for interaction between reinforcement and concrete; embedded element is selected for stirrups; surface-to-surface contact with friction coefficient 0.4 is used for interaction between concrete and steel load transfer plate.

e) Mesh of elements: Abaqus provides different mesh element types depending on the geometry of the model. Use of appropriate mesh element type will make the simulation close to the experimental result of columns, reducing the error between simulation results and the experimental results. With the dimensions of tested columns, all parts of element are meshed with size 10 mm (Figure 6 b).

f) Boundary conditions: support boundary conditions and load boundary conditions in the model are presented in Figure 6 c.

g) Column loading: The loading on the column is carried out by displacement increment assigned on the load transfer plate.

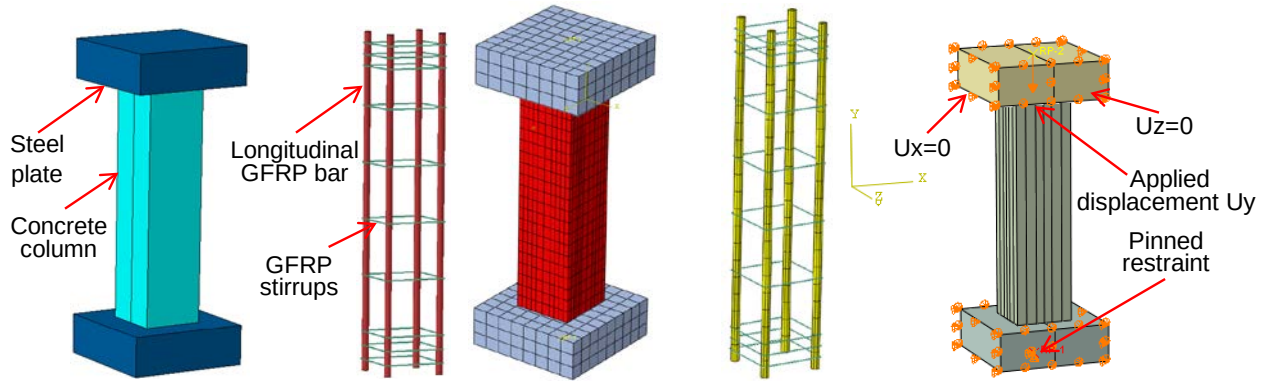

a) Complete model **b) Mesh of elements** **c) Boundary conditions**

Figure 6. Model of short GFRP RC columns in Abaqus.

2.2.2. Verification of numerical models

From the numerical simulation results of GFRP RC columns by aforementioned models, the axial load-strain relationship in concrete at middle of columns curves are established and then comparing with the results obtained from the experiments, these curves are illustrated on Figure 7. Analysis of comparison results on Figure 7 shows a good match between simulation and experiment in all stages of behavior from beginning loading to failure. Failure mode of GFRP RC columns is illustrated on Figure 8. The GFRP bar is considered to be damaged when the stress reaches R_{cf}. Comparing the load-carrying capacity (maximum deviation of 10.5 %), failure modes and load-axial strain curves in concrete between experiment and simulation shows that the simulation method by Abaqus software ensures reliability.

3. Results and Discussion

By using the proven numerical simulation model above, the parametric study on the influence of longitudinal GFRP reinforcement ratios, compressive strengths of concrete and tie spacings on the load-carrying capacity of short GFRP RC columns can be conducted.

3.1. Investigation of contribution of GFRP reinforcement to the load-bearing capacity of RC columns using different concrete strengths (grades)

Contribution of GFRP reinforcement to the load-bearing capacity of RC columns is investigated on specimen 4F12-F6S100 with concrete grades B30, B35, B40, B45 and B60. For these columns, the GFRP reinforcement ratio μ_f and stirrup spacing S are fixed – μ_f = 1.62 % and S = 100 mm. The load-axial strain and load-displacement of these columns from the numerical simulation are shown in Figure 9. When fixing the stirrup configuration, the load-carrying capacity of the column mainly depends on the compressive strength of concrete and the longitudinal GFRP bars, in which concrete strength plays a decisive role. Therefore, when increasing the strength of using concrete, the load-bearing capacity of the column also increases. Accordingly, the load-bearing capacity of the investigated column made from B60 concrete increases 175 % in comparison to that of the column made from concrete B30. However, as the strength of concrete increases, the ductility of the column decreases, which is displayed on the downward branch of the load-displacement curves (Figure 9 b).

The contribution of GFRP bars is defined as the percentage of total axial force in the GFRP bars to maximum load is P_f/P_u, %. In which, P_f depends on the strains in the GFRP bars ε_f at the maximum load and compressive modulus of elastic is $P_f = \varepsilon_f E_{fc} A_f$. The value of ε_f is equal to strain in concrete at maximum stress – i.e. 0.0022 (Figure 3 a). Figure 10 shows the contribution ratio of GFRP bars to total load-carrying capacity of RC columns fabricated from different concrete grades (from B30 to B60). It is clear that contribution of GFRP bars with amount of reinforcement ratio μ_f = 1.62 % to overall load-carrying capacity of RC columns reduces significantly when concrete grade increases from B30 to B60. In GFRP RC columns made from concrete B60, contribution of GFRP bars accounts for 2.74 % and can be ignored. It should bear in mind that this value is only true in this study range (column dimension 150×150 mm, tie spacing 100 mm and diameter of longitudinal GFRP bar 12 mm, GFRP reinforcement ratio μ_f = 1.62 %). Previous studies [4−6, 16, 27] reported that contribution of GFRP reinforcement to load-carrying capacity of GFRP RC columns varies from 3 % to 10 %. However, the research results in this paper show that the contribution of GFRP bars is a variable value depending on many factors such as: concrete strength; GFRP reinforcement ratio; tie spacing etc.

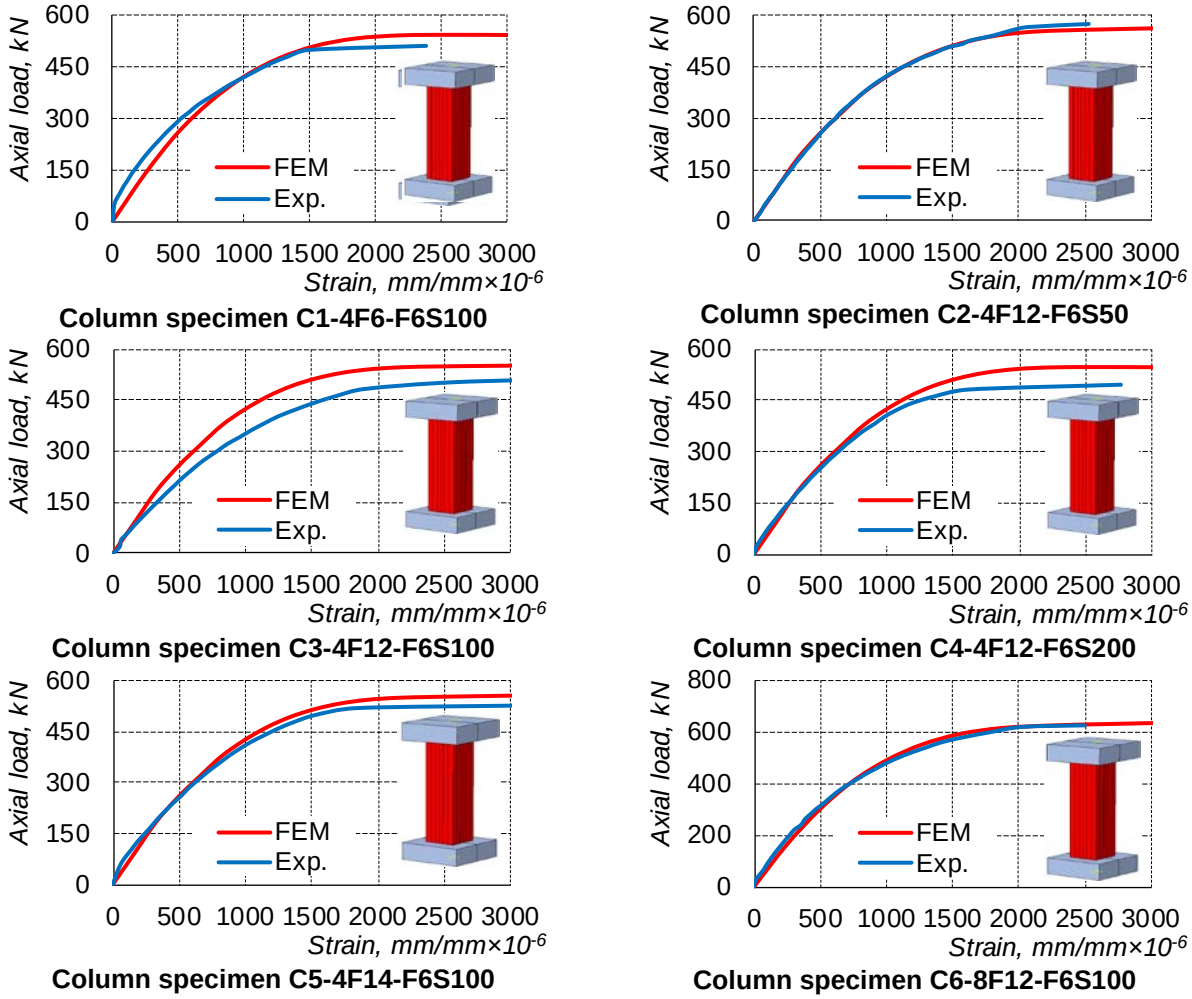

Figure 7. Load versus axial strain in concrete.

Figure 8. Failure mode of GFRP RC column C5-4F14-6S100.

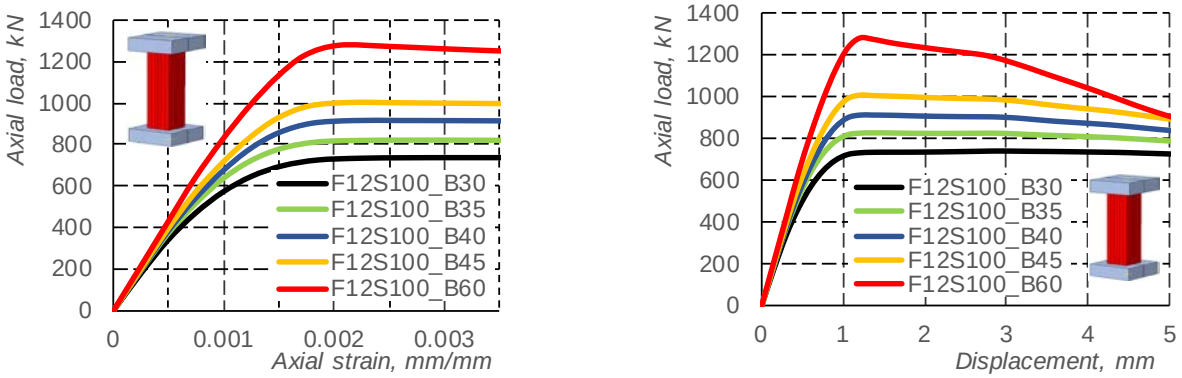

a) Axial load versus axial strain curves **b) Axial load versus displacement curves**

Figure 9. Axial load versus axial strain and displacement curves.

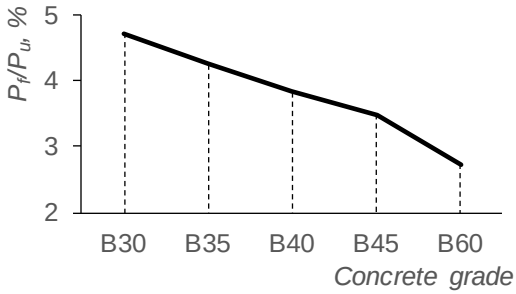

Figure 10. Contribution of GFRP bars to load-carrying capacity of RC columns.

3.2. Influence of tie spacing on load-carrying capacity

Tie spacing significantly influences load-carrying capacity, confinement effect, and failure modes of RC columns. Reducing stirrup spacing can prevent buckling of longitudinal bars, increasing load-carrying capacity. However, smaller stirrup spacing will affect concrete working, causing waste of materials. Design standards always limit the maximum stirrup spacing (S_{max}). According to Vietnamese Design standard 5574:2018 [25] and SP 63.13330.2018 [26], S_{max} should be smaller than 15d (10d) and 400 mm (300 mm) (values in parentheses apply to columns with total reinforcement ratio greater than 3.0 %).

The simulation was conducted on 3 groups of column specimens with longitudinal GFRP reinforcement $4d10$, 4d12 and 4d14, the tie spacing varying from 25 mm to 300 mm. The load-displacement relationship diagrams of investigated columns from numerical simulation are shown in Figure 11, Figure 12 and Figure 13. From these figures, it can be seen that tie spacings mainly affect the inelastic stage of behavior curves of GFRP RC columns. For RC columns with tie spacings greater than 100 mm, in the inelastic stage, the axial load-displacement curve tends to go down. In contrast, for columns with tie spacing of 100 mm or less, after elastic stage, axial load-displacement curve tends to go up and the column still carries loads. Stirrups with small spacing improve flexibility, increase confinement effects of columns and ensure stability of longitudinal GFRP bars, thereby increase the total load-bearing capacity of the columns. Increasing tie spacings leads to decrease in the load-bearing capacity of GFRP RC columns (Figure 14). Particularly, when reducing the tie spacing from 300 mm to 50 mm, the bearing capacity of the columns reinforced with longitudinal bars 4d14, 4d12 and 4d10 increases by 23.3 %, 21.3 % and 12.3 %, respectively. Study results reported by Lotfy [5] indicated that if reducing steel tie spacing from 120 mm to 60 mm, load-carrying capacity of columns reinforced with 4d12 GFRP increases by 20 %. In this study, the same simulation results in an increase by only 11.2 % (after from Fig. 14). This difference could be explained by the fact that Lotfy [5] used steel tie instead of GFRP tie, with better confinement effect than GFRP tie.

Analyzing the load-carrying capacity of RC columns versus tie spacings relationships on Figure 14 shows that, within the study scope, when tie spacing exceeds 16.7d, the bearing capacity of the column almost becomes constant and no longer depends on the tie spacing. This means that the load-bearing capacity of such GFRP RC columns becomes close to that of the plain concrete column. Therefore, in order to take advantage of the bearing capacity of the longitudinal GFRP bars, ensure the simultaneous activation of longitudinal GFRP bars with concrete, it is necessary to limit the tie spacing. It is possible to use the limit of tie spacing according to Vietnamese design standard TCVN 5574:2018 [25] or SP 63.13330.2018 [26], Accordingly, the tie spacing is limited to less than 15d. However, based on the research results of O.S. Al Ajarmeh et al. [24], in order to ensure stability and promote full compressive strength of GFRP bars, it is recommended to limit the tie spacing to less than 8d.

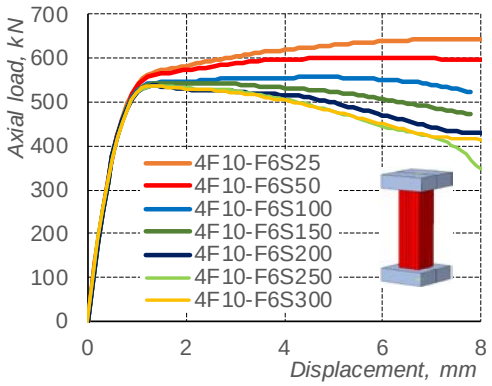

Figure 11. Load versus displacement curves of RC columns 4GFRP10 with different tie spacings.

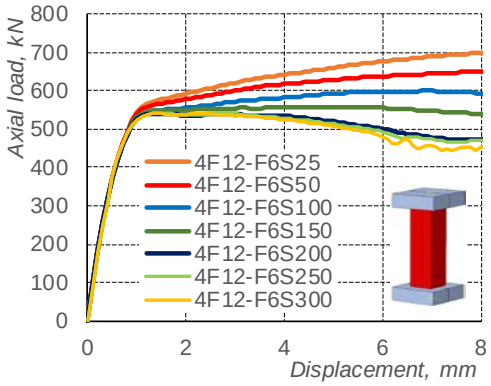

Figure 12. Load versus displacement curves of RC columns 4GFRP12 with different tie spacings.

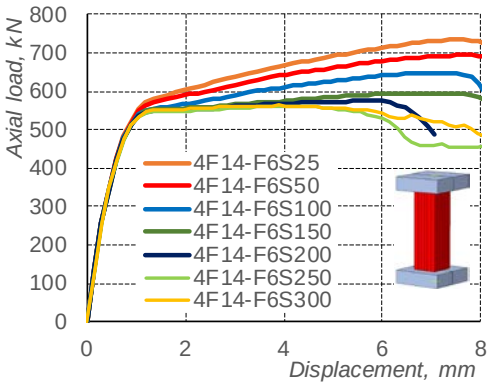

Figure 13. Load versus displacement curves of RC columns 4GFRP14 with different tie spacings.

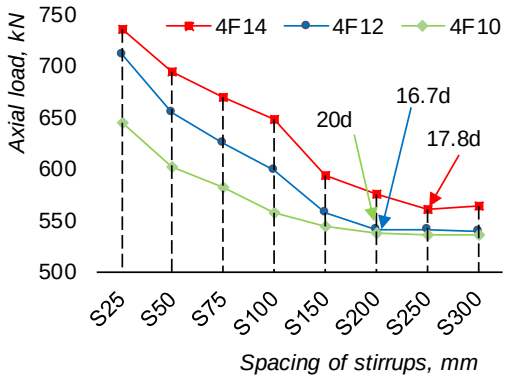

Figure 14. Load-carrying capacity versus tie spacings relationship.

3.3. Influence of GFRP reinforcement ratios on compressive behavior of columns

In order to assess the load-bearing capacity of the GFRP RC columns with a wide range of reinforcement ratios, a numerical study on the behavior of the RC columns with reinforcement ratio varying from μ_f=0.37 % to 3.4 % when fixing the concrete strength R_m=32 MPa and stirrup configuration d6S100 is conducted. Figure 15 shows axial load–displacement of these columns. As mentioned above, load-carrying capacity of GFRP RC columns mainly depends on concrete strength and longitudinal reinforcement. According to the results of numerical study, the load-bearing capacity of columns increases by 29.7 % when the reinforcement ratio increases from μ_f=0.37 % to μ_f =3.24 %. This result is similar to the experimental study of the author [16] and Lotfy [5]. In addition, GFRP longitudinal reinforcement also promotes the flexibility of concrete columns in the inelastic stage (shown in the ascending branches on Figure 15).

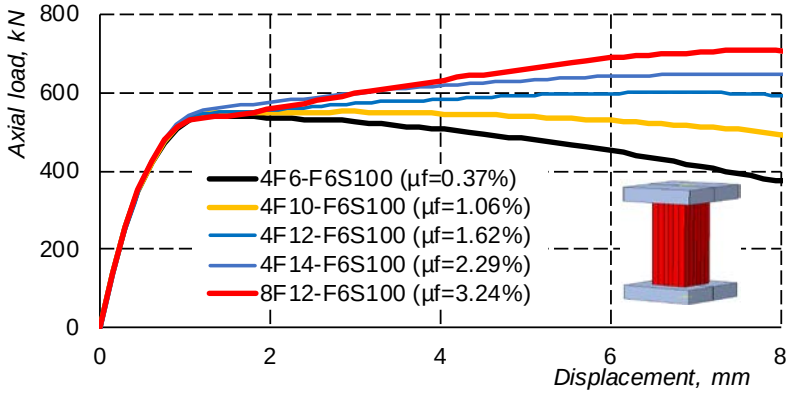

Figure 15. Axial load-displacement curves of GFRP RC columns with different reinforcement ratios.

4. Conclusion

In this study, modeling and verification of behavior of six short concrete columns reinforced with GFRP bars under axial compression load were conducted. By using verified model of GFRP RC columns on Abaqus software, the authors investigated contribution of GFRP bars to load-carrying capacity of RC columns with different concrete grades; the influence of tie spacing on load-bearing capacity and the behavior of GFRP RC columns when increasing GFRP reinforcement ratios. Based on the numerical simulation results presented in this study, the following conclusions can be drawn:

1. Numerical simulation model of GFRP RC columns based on CDP model and the linear stress-strain relationship of GFRP bars gives similar results to the experiment. Therefore, the proposed simulation technique of columns is reliable and can be used for parametric study;

2. Using the compressive strength of GFRP bar equal to about 60 % of the tensile strength when Lf/df≤8 and additional reduction coefficient when Lf/df> 8 for numerical simulation model of GFRP RC columns gives consistent results with experimental values;

3. - Concrete strength significantly influences the load-bearing capacity and the behavior of the GFRP RC columns in both elastic and nonlinear stages. Using high-strength concrete reduces ductility of the column and decreases the contribution of GFRP bars to load-carrying capacity of columns. Changing the class of

concrete from B30 to B60 leads to a decrease in the contribution to load-bearing capacity of columns from 4.73 % to 2.74 %;

4. - Tie spacing greatly affects the bearing capacity and behavior of the column, especially in the nonlinear stage. Reducing the tie spacing increases the flexibility of the column, the confinement effect and the stability of the longitudinal GFRP bars, thereby increases the bearing capacity of the columns. From parametric study results in this paper, it is recommended that the maximum tie spacing in GFRP RC columns should be smaller than 8d;

5. - Increase of longitudinal GFRP reinforcement ratio improves the bearing capacity and ductility of the columns.

References

1. Uğur, A., Unal, A., Akgöbek, B., Kamanli, M., Cengiz, S. Use of GFRP Bar in Civil Engineering. 4th International Symposium on Innovative Approaches in Engineering and Natural Sciences. 2019. Pp. 95–100. DOI: 10.36287/setsci.4.6.029
2. Husain, S.F., Shariq, M., Masood, A. GFRP bars for RC structures – A Review. International Conference on Advances in Construction Materials and Structures (ACMS-2018). 2018. (March).
3. Alsayed, S.H., Al-Salloum, Y.A., Almusallam, T.H., AMJAD, M.A. Concrete Columns Reinforced by GFRP Rod. Fourth International Symposium on Fiber-Reinforced Polymer Reinforcement for Reinforced Concrete Structures. 1999. Pp. 103–112.
4. Luca, A., Matta, F., Nanni, A. Behavior of Full-Scale Glass Fiber-Reinforced Polymer Reinforced Concrete Columns under Axial Load. ACI Structural Journal. 2010. 107. Pp. 589–596.
5. Lotfy, E. Nonlinear analysis of Reinforced Concrete Columns with Fiber Reinforced Polymer Bars. World Journal of Engineering. 2011. 8(4). Pp. 357–368. DOI: 10.1260/1708-5284.8.4.357
6. Tobbi, H., Farghaly, A.S., Benmokrane, B. Concrete columns reinforced longitudinally and transversally with glass fiber-reinforced polymer bars. ACI Structural Journal. 2012. 109(4). Pp. 551–558. DOI:10.14359/51683874.
7. Mohamed, H.M., Afifi, M.Z., Benmokrane, B. Performance evaluation of concrete columns reinforced longitudinally with FRP bars and confined with FRP hoops and spirals under axial load. Journal of Bridge Engineering. 2014. 19(7). Pp. 1–12. DOI: 10.1061/(ASCE)BE.1943-5592.0000590
8. Afifi, M.Z., Mohamed, H.M., Chaallal, O., Benmokrane, B. Confinement model for concrete columns internally confined with carbon FRP spirals and hoops. Journal of Structural Engineering (United States). 2015. 141(9). Pp. 1–11. DOI: 10.1061/(ASCE)ST.1943-541X.0001197
9. Pateriya, R., Akhtar, S., Rajvaidya, P.N. Analysis of Compressive Strength of Columns Reinforced with Steel & FRP Bars. 2015. 4(6). Pp. 4–8.
10. Hadi, M.N.S., Karim, H., Sheikh, M.N. Experimental Investigations on Circular Concrete Columns Reinforced with GFRP Bars and Helices under Different Loading Conditions. Journal of Composites for Construction. 2016. 20(4). Pp. 1–12. DOI: 10.1061/(ASCE)CC.1943-5614.0000670
11. Tu, J., Gao, K., He, L., Li, X. Experimental study on the axial compression performance of GFRP-reinforced concrete square columns. Advances in Structural Engineering. 2019. 22(7). Pp. 1554–1565. DOI: 10.1177/1369433218817988
12. Turvey, G., Zhang, Y. A computational and experimental analysis of the buckling, postbuckling and initial failure of pultruded GRP columns. Computers & Structures – COMPUT STRUCT. 2006. 84. Pp. 1527–1537. DOI: 10.1016/j.compstruc.2006.01.028
13. Nunes, F., Correia, M., Correia, J.R., Silvestre, N., Moreira, A. Experimental and numerical study on the structural behavior of eccentrically loaded GFRP columns. Thin-Walled Structures. 2013. 72. Pp. 175–187. DOI: 10.1016/j.tws.2013.07.002
14. Tao, P.Z., Wang, Z.-B., Yu, Q. Finite element modelling of concrete-filled steel stub columns under axial compression. Journal of Constructional Steel Research. 2013. 89. Pp. 121–131. DOI: 10.1016/j.jcsr.2013.07.001
15. Elchalakani, M., Ma, G., Aslani, F., Duan, W. Design of GFRP-reinforced rectangular concrete columns under eccentric axial loading. Magazine of Concrete Research. 2017. 69(17). Pp. 865–877. DOI: 10.1680/jmacr.16.00437
16. Duy, N.P., Anh, V.N., Minh, N., Anh, T., Eduardovich, P.A. Load-Carrying Capacity of Short Concrete Columns Reinforced with Glass Fiber Reinforced Polymer Bars Under Concentric Axial Load. International Journal of Engineering and Advanced Technology. 2019. 9(2). Pp. 1712–1719. DOI: 10.35940/ijeat.b2372.129219
17. FIB (International Federation for Structural Concrete). Fib Model Code for Concrete Structures 2010. Ernst & Sohn, a Wiley brand, 2013.
18. Lubliner, J., Oliver, J., Oller, S., Oñate, E. A plastic-damage model for concrete. Int. J. Solids and Structures. 1989.
19. Lee, J., Fenves, G.L. Plastic-damage model for cyclic loading of concrete structures. Journal of engineering mechanics. 1998. 124(8). Pp. 892–900.
20. Alfarah, B., López-Almansa, F., Oller, S. New methodology for calculating damage variables evolution in Plastic Damage Model for RC structures. Engineering Structures. 2017. 132. Pp. 70–86.
21. FRP Vietnam JSC. Technical Specifications of GFRP. Viet Nam 2014.
22. Lucier, G. Tension Tests of GFRP Bars (Prepared for: Fiber reinfor plymer Vietnam) 2014.
23. Khan, Q.S., Sheikh, M.N., Hadi, M.N.S. Tension and compression testing of fibre reinforced polymer (FRP) bars. The 12th Iternational Symposium on FIber Reinforced Polymers for Reinforced Concrete Structures (FRPRCS-12). 2015. Pp. 1–6.
24. AlAjarmeh, O.S., Manalo, A.C., Benmokrane, B., Vijay, P.V., Ferdous, W., Mendis, P. Novel testing and characterization of GFRP bars in compression. Construction and Building Materials. 2019. 225. Pp. 1112–1126. DOI: 10.1016/j.conbuild-mat.2019.07.280.
25. IBST. TCVN 5574:2018 Concrete and reinforced concrete structures - Design standard2018.
26. NIIZHB imeni A.A. Gvozdeva. SP 63.13330.2018 Concrete and Reinforced Concrete Structures. General provisions 2018.
27. Fillmore, B., Sadeghian, P. Contribution of longitudinal glass fiber-reinforced polymer bars in concrete cylinders under axial compression. Canadian Journal of Civil Engineering. 2018. 45(6). Pp. 458–468. DOI: 10.1139/cjce-2017-0481

Contacts:

Nguyen Phan Duy, nguyenphanduy@muce.edu.vn
Vu Ngoc Anh, vungocanh@muce.edu.vn
Dang Vu Hiep, dangvuhiep2009@yahoo.com
Nguyen Minh Tuan Anh, nguyenminhtuananh@muce.edu.vn